Hydrol. Earth Syst. Sci. Discuss., 11, 12405–12441, 2014
www.hydrol-earth-syst-sci-discuss.net/11/12405/2014/
doi:10.5194/hessd-11-12405-2014

Hydrology and Earth System Sciences
Open Access
Discussions

Groundwater surface mapping informs sources of catchment baseflow

J. F. Costelloe[1], **T. J. Peterson**[1], **K. Halbert**[2], **A. W. Western**[1], **and J. J. McDonnell**[3]

[1]Department of Infrastructure Engineering, University of Melbourne, Australia
[2]Ecole Centrale de Nantes, Nantes, France
[3]School of Environment and Sustainability, University of Saskatchewan, Canada

Received: 13 October 2014 – Accepted: 15 October 2014 – Published: 5 November 2014

Correspondence to: J. F. Costelloe (jcost@unimelb.edu.au)

Published by Copernicus Publications on behalf of the European Geosciences Union.

Groundwater surface mapping informs sources of catchment baseflow

J. F. Costelloe et al.

Abstract

Groundwater discharge is a major contributor to stream baseflow. Quantifying this flux is difficult, despite its considerable importance to water resource management and evaluation of the effects of groundwater extraction on streamflow. It is important to be able to differentiate between contributions to streamflow from regional groundwater discharge (more susceptible to groundwater extraction) compared to interflow processes (arguably less susceptible to groundwater extraction). Here we explore the use of unconfined groundwater surface mapping as an independent dataset to constrain estimates of groundwater discharge to streamflow using traditional digital filter and tracer techniques. We developed groundwater surfaces from 98 monitoring bores using Kriging with external drift. Baseflow estimates at the catchment outlet were made using the Eckhardt digital filter approach and tracer data mixing analysis using major ion and stable isotope signatures. Our groundwater mapping approach yielded two measures (percentage area intersecting the land surface and monthly change in saturated volume) that indicated that digital filter-derived baseflow significantly exceeded probable groundwater discharge during the high flow period of spring to early summer. Tracer analysis was not able to resolve contributions from ungauged tributary flows (sourced from either shallow flow paths, i.e. interflow and perched aquifer discharge, or regional groundwater discharge) and regional groundwater. Groundwater mapping was able to identify ungauged sub-catchments where regional groundwater discharge was too deep to contribute to tributary flow and thus where shallow flow paths dominated the tributary flow. Our results suggest that kriged unconfined groundwater surfaces provide a useful, empirical and independent dataset for investigating sources of fluxes contributing to baseflow and identifying periods where baseflow analysis may overestimate groundwater discharge to streamflow.

HESSD

11, 12405–12441, 2014

1 Introduction

Groundwater discharge is a major contributor to stream baseflow. Quantifying this flux is of considerable importance to water resource management (Woessner, 2000; Sophocleous, 2002; Cartwright et al., 2014). In recent decades there have been dramatic increases in the extraction of groundwater for agricultural use, driven by factors such as expansion of irrigated agriculture in south Asia (Llamas and Martínez-Santos, 2005; Perrin et al., 2011) and long-term drought in southeastern Australia (Leblanc et al., 2012; van Dijk et al., 2013). It has been long recognised that over-extraction from aquifers may result in significant long-term declines in groundwater levels and hence decreases in baseflow to rivers (Sophocleous, 2000, 2002). As a result, the switch to groundwater as a source of irrigation supply has the potential to exacerbate decreases in baseflow in rivers already experiencing reductions in flow from drought or instream water use. Whilst these generalities of groundwater extraction and stream baseflow reduction are clear, the particularities for any given catchment are complex and difficult to quantify. The separation of contributions from regional unconfined groundwater to streamflow versus other baseflow generation processes (e.g. interflow, bank storage return, perched aquifer discharge) is technically difficult but fundamentally important for quantifying how regional groundwater extraction may affect baseflow in rivers (Wittenberg, 1999). Despite decades of work (e.g. Nathan and McMahon, 1990; Tallaksen, 1995; Wittenberg, 1999; Eckhardt, 2005) methods to quantify and discriminate between "slow flow" (itself a poorly defined term) contributions to the stream using only streamflow data are approximate at best.

In its simplest form, the baseflow component of streamflow is the sum of the slow flow pathways into the river (Ward and Robinson, 2000). Regional, unconfined groundwater (often termed "deep groundwater") can discharge into the river via the valley floor or through more shallow, lateral flow paths, such as discharge into tributaries draining the valley slopes. Interflow pathways can also contribute to tributary streamflow and recent work has shown a continuum between groundwater and interflow processes (sometimes referred to as "shallow groundwater" in hilly terrains) along the stream reach (Jencso et al., 2009; Jencso and McGlynn, 2011). In terms of water resource extraction (e.g. for urban supplies or irrigation on the valley floor), groundwater pumping typically targets the deep groundwater and often in alluvial valley locations where the depth to groundwater is at a minimum. Thus, it is important to be able to differentiate between contributions to streamflow from deep groundwater discharge (more susceptible to groundwater extraction) compared to interflow processes (arguably less susceptible to groundwater extraction).

But how can the baseflow components be identified? Digital recursive filters are the most common method of separating baseflow from streamflow but do not discrimate between the different components of baseflow and the estimate is integrated over the entire catchment area upstream of the gauging station. The technique rests on the assumption that baseflow is comprised of linear or non-linear outflow from an aquifer (e.g. Nathan and McMahon, 1990; Wittenberg, 1999; Eckhardt, 2005). All of the filter approaches require calibration of 1–3 parameters based on subjective criteria (e.g. recession curve analysis, typical values, etc). Calibration of these parameters against synthetic baseflow derived from a numerical model has shown that optimal values vary considerably with catchment and climatic characteristics, many of which are not known or not possible to know a priori for natural catchments (Li et al., 2014). There is typically significant variability in recession curves from a given catchment suggesting a range of processes and flow paths (e.g. deep and shallow groundwater flowpaths, interflow, bank storage) affecting baseflow (Tallaksen, 1995). The regional unconfined groundwater may drive only some of this response (Cartwright et al., 2014) and additional stores and pathways can be contributing to baseflow (Jencso and McGlynn, 2011; Chen and Wang, 2013). The variable, often non-linear, baseflow response has been attributed to additional processes affecting the groundwater discharge, such as phreatic evapotranspiration (Wittenberg and Sivapalan, 1999) and recharge from soils or perched aquifers (Fenicia et al., 2006; Jencso and McGlynn, 2011). Baseflow analysis using digital recursive filters typically does not use groundwater data to constrain or test the

HESSD
11, 12405–12441, 2014

estimates, even though baseflow should vary systematically with groundwater levels (Gonzalez et al., 2009; Meshgi et al., 2014), although more use is being made of tracer data for this purpose (e.g. Cartwright et al., 2014).

Tracer data are also commonly used to estimate groundwater discharge to streams (Cook et al., 2003; McGlynn and McDonnell, 2003; Cartwright et al., 2011; Atkinson et al., 2014) and rely on the assumption that different contributors to streamflow have distinctive and invariant chemical, isotopic or radiogenic end-member signatures that can be apportioned in the streamflow mixture (McCallum et al., 2010). Insights have been gained by heavily instrumenting catchments to increase confidence in the identification of sources and pathways of the fluxes being measured – but this is usually feasible only on small experimental catchments or hillslopes (Kendall et al., 2001). In larger catchments utilised for water use, it can be difficult to separate fluxes of interest due to similarities in the tracer signatures, such as between surface flow and interflow (Kendall et al., 2001) or bank storage discharge and streamflow (McCallum et al., 2010). This problem can been addressed by using a multiple tracer approach, so that a mix of isotopic and ionic data or conservative and radiogenic data can provide independent information on sources and pathways within a catchment (Cook et al., 2003; Cartwright et al., 2011; Atkinson et al., 2014). However, field studies are rarely able to identify end-members for all flow paths of interest and deep and shallow groundwater fluxes are commonly lumped together.

Digital recursive filters and tracer-based analysis measure different components of baseflow and provide different bounds to the estimation of groundwater discharge. For instance, digital filter analysis provides an upper bound to groundwater discharge, integrated over the upstream catchment area. Tracer analysis can provide more spatially explicit estimates of groundwater discharge but can struggle with separating discharge from deep groundwater flowpaths compared to shallow, lateral groundwater flowpaths. Here we argue that additional datasets on groundwater dynamics are of benefit in better constraining regional groundwater discharge estimates determined by these traditional methods. One overlooked measure available in many catchments is groundwater

HESSD
11, 12405–12441, 2014

level data. Intuitively, such data are directly relatable to the groundwater discharge component of baseflow (Gonzalez et al., 2009; Meshgi et al., 2014). More importantly, we hypothesize that groundwater observations provide complementary, independent time-series of data on the dynamics of the groundwater–surface water interaction.

The use of groundwater level data at the reach or catchment scale faces a number of challenges, principally that these data are sporadically available in time and space. To understand the spatial variability of groundwater throughout a catchment, various geostatistical techniques have been developed to interpolate sparse groundwater level observations (Desbarats et al., 2002; Boezio et al., 2006; Lyon et al., 2006). However, to date, maps have been derived for the average groundwater level at each bore, rather than instantaneous levels (Desbarats et al., 2002), or at a specific time using either continuous water level observations (Boezio et al., 2006; Lyon et al., 2006) or basic hydrograph interpolation methods (Peterson et al., 2011) that ignore the variability between observation times. Considering that groundwater observations are most often collected manually and are rarely coincident across a catchment, using groundwater maps to inform groundwater–surface water interaction requires maps for specific time points and hence a hydrograph interpolation technique that, idealy, accounts for the variability between observations. Recently, Peterson and Western (2014) developed such an interpolation approach for irregularly spaced observations that now allows for daily interpolated observations to be generated for the estimation of groundwater surfaces for any given date. This new method enables the generation of high frequency groundwater surfaces from operational monitoring bore networks, which opens up a possible new way forward for estimating groundwater contributions to baseflow.

Here we investigate how groundwater head data, amalgamated as water table maps using the new Peterson and Western (2014) temporal interpolation combined with the Peterson et al. (2011) spatial interpolation approach, can be used as an independent and generally available dataset to constrain estimates of groundwater discharge to streamflow using traditional digital filter and tracer techniques. We focus on a humid catchment in southeastern Australia where substantial groundwater data have been

HESSD
11, 12405–12441, 2014

collected arising from investigations of groundwater extraction for urban water supply (SKM, 2012) and river damming. We combine 44 years of streamflow and groundwater data observations from 98 monitoring bores across the 311 km^2 catchment to investigate the utility of the groundwater data for informing sources of catchment baseflow. We test three hypotheses:

1. variations in baseflow can be explained by variations in the areas of very shallow water tables (i.e. direct discharge areas),
2. variations in baseflow can be explained by changes in saturated volume between monthly water table surfaces,
3. water table mapping can identify whether ungauged tributary inflow is driven by regional groundwater discharge.

2 Methods

2.1 Study area

The Gellibrand River catchment is located in southeastern Australia in the Otway Ranges. It has a perennial, highly seasonal flow regime and a humid climate (rainfall of 1000 mm a^{-1}). The Gellibrand River is dominated by a constrained valley with much of the study reach being forested by cool temperate eucalypt rainforests, except for cleared grazing areas along the valley floor. The catchment is well gauged with gauging stations at upper Gellibrand and Bunker Hill on the Gellibrand River and gauging stations measuring flow in two of the larger tributaries (Love Creek and Lardner Creek, Fig. 1). The catchment has an area of 311 km^2 to a mid-catchment gauging station at Bunker Hill. Comparison of potentiometric groundwater data to river levels indicates mostly gaining conditions along the Gellibrand River (SKM, 2012; Atkinson et al., 2014).

The southern half of the catchment, which includes the upper reaches of the Gellibrand River and coincides with steep, forested terrain, is underlain by the volcanogenic sandstones, siltstones and mudstones of the Cretaceous Otways Group (Fig. 1), which forms the basement to the catchment. Relatively few bores occur within this unit in the Gellibrand catchment. The more open, alluvial valley of the Gellibrand is underlain predominantly by fluvial sands with interbedded silts and clays of the late Cretaceous Wangerrip Group and overlying Quaternary alluvium. This area contains the most bores and is considered as the primary aquifer in the region (Atkinson et al., 2014). The northern half of the catchment, particularly the Love Creek sub-catchment, is underlain by the marine calcareous clays of the Miocene Heytesbury Group that confine the underlying aquifers in the Wangerrip Group. A number of bores occur in this area but are mainly screened within the main aquifer (Eastern View Formation) of the underlying Wangerrip Group.

2.2 Groundwater monitoring and mapping

Ninety-eight groundwater monitoring bores in and around the boundary of the Gellibrand catchment were identified and water level data were extracted from the Victorian Groundwater Management System (http://www.vvg.org.au/cb_pages/gms.php). The area contains a relatively large number of monitoring bores due to earlier investigations for a potential damming of the Gellibrand River and also extraction of groundwater for urban water supply (SKM, 2012). In order to construct water table maps for specified dates, the periodic (generally monthly) water level observations of the bore data were first modelled using the nonlinear transfer-function-noise time-series modelling methodology of Peterson and Western (2014). Water level estimates for the start of each month were then derived by adding the time-series simulation, interpolated to the required data, to a univariate oridinary kriging estimate of the timeseries model error at the required date, which ensured a zero error at dates with a water level observation. Water table maps were then produced for the first of each month for the years 2007 to 2010 using the Kriging with external drift method (Peterson et al., 2011). In applying

HESSD
11, 12405–12441, 2014

the Kriging with external drift, the external drift term was the land surface elevation (Shuttle Radar Terrain Model (SRTM) 30 m dataset). A model variogram was derived for the component of the groundwater elevation not explained by the external drift. This groundwater level component was first estimated using ordinary least squares regression and then minimised by repeatedly fitting an isotropic exponential variogram, using multi-start Levenberg–Marquardt optimization and re-derivation of the water level component, until a stable model variogram was achieved. The depth to water table was calculated by difference from the SRTM representation of the ground surface and used to measure changes in the percentage of the catchment with very shallow water tables (nominally "saturated") over the period of mapping. This was done for the parts of the catchment with an elevation of < 100 m in order to analyse changes in the saturated area around the valley floor and lower slopes of the catchment where most monitoring bores were located and hence confidence in the water table mapping was highest. Five threshold depths to the water table (0, 0.25, 0.50, 0.75, 1.0 m) were used to determine changes between the seasonal maximum (spring) and minimum (autumn) saturated areas. The threshold depths were not calibrated but were arbitrarily chosen to capture some of the uncertainty in the water table position as mapped for each month. In addition, changes in total volume below the water table (i.e. volume containing sediments and pore spaces) between months were calculated using the water table maps, again using the catchment area below 100 m elevation.

2.3 Digital recursive filter analysis of baseflow

The Eckhardt (2005) two parameter, digital recursive filter was used to produce baseflow time-series for the Gellibrand streamflow record at the Bunker Hill gauging station (Station number 235227). The Eckhardt filter separates the slow flow component of the stream hydrograph based on the groundwater discharge being linearly proportional to the unconfined aquifer storage. This filter was chosen as it has a physical basis and produces results comparable with other digital recursive filters (Eckhardt, 2008). The α parameter (representing the recession constant of streamflow) was determined by

HESSD
11, 12405–12441, 2014

the 95th percentile upper bound of the scatter plot of daily discharge (Q_k) against discharge from the next day (Q_{k+1}). These data points were extracted for recession flows of five days or longer (see Eckhardt, 2008) below a selection of percentiles of total flows (i.e. 30th, 40th, 50th). The BFI_{max} parameter (representing the maximum value of the baseflow index, i.e. baseflow/total streamflow, that can be modelled by the filter algorithm) was chosen to minimize periods of baseflow greater than observed streamflow. Time-series of baseflow were then defined using the selected pairs of parameter values to represent a possible envelope of baseflow for the study catchment.

2.4 Hydrochemical sampling and analysis

Water samples from streamflow were collected by automatic samplers (ISCO) at several locations in the catchment, including upstream (Upper Gellibrand gauging station and Sayers Bridge, see Fig. 1) and downstream (Bunker Hill gauging station) locations from the Gellibrand River and from major tributaries in January and June 2013. Grab samples were also collected from smaller, ungauged tributaries and from the Gellibrand River during the sampling period and also in December 2013. Unconfined groundwater samples were taken from bores in the alluvial area of the Gellibrand River (some data supplied by Alex Atkinson, Monash University, see Atkinson et al., 2014) after purging 2–3 well volumes of bores or until field water parameters (e.g. electrical conductivity, pH, temperature) had stabilised. Samples were filtered through a 0.45 µm membrane filter and the cation aliquots were further acidified to pH < 2 using 1 M HNO_3 and stored at 4 °C until analysis at the Research School of Earth Science laboratory, Australian National University. Cation analyses were performed by ICP mass spectrometry (Varian Vista AX CCD Simultaneous ICP-OES) and anion analysis performed by ion chromotography (Dionex Series 4500i). Colourimetric alkalinity titrations were performed using a Hach® field titration kit. Stable isotope ratios were measured at the University of Melbourne by laser spectroscopy (Picarro cavity ringdown spectrometer). Isotope ratios are reported to known values of a series of in-house standards that were initially individually calibrated to International Atomic Agency Standards (IAEA) Vienna Standard

HESSD
11, 12405–12441, 2014

Mean Ocean Water (VSMOW) (0.0 ‰ δ^{18}O, 0.0 ‰ δ^{2}H), Greenland Ice Sheet Precipitation (GISP) (−24.8 ‰ δ^{18}O, −189.5 ‰ δD) and Standard Light Antarctic Precipitation 2 (SLAP2) (−55.5 ‰ δ^{18}O, −427.5 ‰ δD). Three repeat samples were run per batch to evaluate reproducibility. The instrument precision of the Picarro is 0.3 ‰ for δD and 0.1 ‰ for δ^{18}O.

Mass balance calculations were conducted on the streamflow samples using selected ions (Cl, Na, Ca, Mg) and stable isotopes (^{18}O, ^{2}H) using a multiple end-member model. The hydrochemical samples included upstream and downstream (gauged) locations on the Gellibrand River, major gauged tributaries and a range of smaller, ungauged tributaries. The mass balance for a gaining reach is defined by the load (1) and the discharge (2).

$$Q_{ds}C_{ds} = Q_{us}C_{us} + Q_{gw}C_{gw} + Q_{ut}C_{ut} + Q_{gt}C_{gt} \quad (1)$$

$$Q_{ds} = Q_{us} + Q_{gw} + Q_{ut} + Q_{gt} \quad (2)$$

Where Q is discharge and C is concentration and the subscripts refer to; ds – downstream Gellibrand (Bunker Hill gauging station), us – upstream Gellibrand, gw – groundwater, ut – ungauged tributaries, gt – gauged tributaries. The unknowns in the above equations are Q_{gw} and Q_{ut} and to solve require two sets of concentrations, or a single tracer with data over two or more days. This approach accounts for the contribution from the alluvial groundwater in the reach between the Upper Gellibrand and Bunker Hill gauging stations.

3 Results

We first analyse the baseflow characteristics of the river using the Eckhardt (2005) baseflow filter. Second, the streamflow chemical and isotopic patterns are presented and third, mass balance analysis is used to estimate groundwater discharge and ungauged tributary discharge. Finally, using the results of mapping the unconfined

HESSD
11, 12405–12441, 2014

groundwater surfaces, we analyse relationships between the three datasets (groundwater surfaces, baseflow filter estimates, mass balance tracer estimates) and explore how the groundwater surfaces can be used to constrain estimates of groundwater discharge derived from ionic mass balance and baseflow filter analyses.

3.1 Baseflow analysis

The Eckhardt baseflow estimates produce patterns that follow the highly seasonal pattern shown by the overall river discharge and indicated that baseflow significantly contributed to overall streamflow (Fig. 2). The α parameter values declined moderately as the threshold flow percentile value to define recession periods increased (30th – 0.990, 40th – 0.988, 50th – 0.985). The BFI_{max} parameter values that minimized periods of baseflow greater than streamflow clustered around 0.2 but showed slight increases as α decreased (30th – 0.20, 40th – 0.20, 50th – 0.22). This method used for determining the BFI_{max} parameter produced values below the recommended range (~ 0.8 for perennial rivers with porous aquifers, Eckhardt, 2005) and lie closest to the recommended BFI_{max} value (0.25) for perennial rivers with hard rock aquifers. The filtered baseflow time-series produced mean monthly BFI estimates of 0.54–0.64 during the summer–autumn period (January–May) and 0.26–0.30 during the winter–spring period (June–November).

3.2 Streamflow chemistry and stable isotope patterns

Streamflow and groundwater samples of the Gellibrand catchment have similar Na–Cl–HCO_3 compositions (Supplement A) and are further examined using a Piper diagram (Fig. 3). The upstream, downstream and major tributary flow compositions plot closely together, with the downstream composition showing a shift towards the alluvial groundwater composition, relative to the upstream composition. However, seasonal changes in streamflow chemistry are also apparent with winter samples (June 2013) plotting closer to the groundwater composition (higher Cl, lower HCO_3) in comparison to the summer low flow samples (January and December 2013). The ungauged (minor) tributary samples show a greater spread in compositions, with only the largest of the ungauged tributaries (Charley's Creek, 47.4 km^2) plotting with the gauged streamflow (Gellibrand, Love, Lardner), and others plotting in and around the alluvial groundwater compositions. The Charley's Creek subcatchment drains the southern half of the catchment underlain by the Otways Group and has a relatively similar area to the two gauged tributaries (Lardner Creek 51.8 km^2, Love Creek 76.6 km^2). The ungauged tributaries show a greater spread in composition than the alluvial groundwater but this was dominated by relatively high Mg and SO_4 concentrations in two tributaries whilst the other tributaries were slightly depleted in Ca and K compared to the alluvial groundwater. The Love Creek samples have significantly higher ionic concentrations than all other streamflow samples in the catchment (Supplement A) but have similar ionic ratios, as shown by plotting closely to the gauged streamflow samples in Fig. 3.

The stable isotope data show that the winter streamflow samples (e.g. June 2013) were more depleted than summer (e.g. January 2013) samples with the early summer (December 2013) samples having intermediate values (Fig. 4). This indicates either a short residence time (i.e. streamflow samples match a seasonal shift in rainfall isotopic signal) or a shift in the mix of sources of streamflow. The mean Global Network of Isotopes in Precipitation (GNIP) Melbourne winter rainfall signature is $\delta^{18}O$ of −5.6 ‰ and δ^2H of −33.5 ‰ while the mean summer rainfall signature is $\delta^{18}O$ of −3.5 ‰ and δ^2H of −16.6 ‰ (http://nucleus.iaea.org/CIR/CIR/GNIPIHIS.html). Compared to the seasonal shift in isotopic signature (Fig. 4), there was not much differentiation within individual trips between upper and lower catchment or major and minor tributaries (data not separated by criteria in Fig. 4). For the winter sampling period, all of the streamflow samples plot more closely to alluvial groundwater samples compared to the summer samples.

The dominance of the contribution of groundwater discharge to streamflow during summer low flow periods was also investigated by examining how tracer values changed during the recession of flow events during the summer (January 2013) sampling period (Fig. 5). In general, only the chloride data showed an approximately linear increase in concentration that would be expected if the groundwater discharge flux contributed proportionally more to streamflow during the short-term recession. The other major ions (e.g. Na, Ca, Mg) and isotope values remained relatively consistent or showed a variable pattern over time during the flow recession. In addition, the streamflow composition remains distinct from the groundwater composition even during the summer low flow periods (Figs. 3 and 4). These patterns suggest that other end-member fluxes need to be considered during the flow recession rather than a simple two end-member system (i.e. upstream streamflow and groundwater discharge).

The compositional similarities of the ungauged streamflow samples to the alluvial groundwater samples, compared to the gauged streamflow samples, raises the question whether the minor ungauged tributaries represent discharged groundwater. Alternatively, the ungauged streamflow may be driven by perched aquifer or similar interflow type processes. If the ungauged tributary samples represent a distinct source from the regional groundwater, then their chemical similarity to the groundwater samples could result in chemical mass balance techniques that do not consider the contribution from ungauged tributaries, overestimating the groundwater contribution to streamflow (Sect. 3.3).

3.3 Mass balance analysis

Mass balances were calculated using Cl, Na, Ca, Mg, ^{18}O and ^{2}H results from samples collected in January, June and December 2013 (Table 1). The January 2013 period covered a consistent recession period (see Fig. 5) while the June 2013 period included a flow event midway through the sampling period. The December 2013 sampling covered a two day "snapshot" during a recession period.

In January 2013, the selected ions showed similar downstream (i.e. Sayers Bridge to Bunker Hill) percentage increases (62–82 %) during the recession events and cross plots (not shown) indicated that Na, Ca and Mg were showing conservative behavior relative to Cl. The stable isotope data showed smaller percentage changes (1–11 %)

HESSD
11, 12405–12441, 2014

to more depleted values moving downstream. The mass balance analysis (Table 1) showed that the groundwater discharge term generally dominated during this period of low flow (particularly using two end-member analysis) but that the ungauged tributary discharge could also be a significant term, even during summer low flow conditions. This was consistent with field observations that a number of the larger ungauged tributaries were flowing in January 2013. A number of combinations of end-members could not return physically realistic estimates (i.e. one discharge term being negative). For the single end-member, time-series analysis, the estimates with groundwater dominating did not reach an optimal solution because of the constraint that the tributary inflow could not be negative.

In June 2013, before and after a flow event, the selected ions showed more variable downstream (i.e. Upper Gellibrand to Bunker Hill) percentage increases (57–124 %) while the stable isotopes did not show any consistent pattern between upstream and downstream flow. The resulting mass balance analyses showed a range of contributions from the groundwater discharge and ungauged tributary flow terms (Table 1). The single and double end-member, time-series analyses did not reach an optimal solution, with either the tributary inflow or groundwater discharge term being limited by the non-negative flux constraint.

The mass balance analyses indicated that the ungauged tributary flow term was often significant (consistent with field observations) but difficult to separate from the groundwater discharge term. This was likely due to the similarity in signature between these two end-members. There was also significant variation within each of the end-member compositions and the use of mean concentrations in the mass balance analyses is likely to contribute to the uncertainty in flux estimates.

3.4 Baseflow – water table dynamics

The monthly time-series of water table mapping allows analysis of the dynamics of the relationship between baseflow and water table fluctuations and of the spatial distribution of shallow water table relative to the sampling of ungauged tributaries.

HESSD
11, 12405–12441, 2014

Water table maps showed that areas with the water table ≤ 1 m from the ground surface were confined to the alluvial plains of the Gellibrand River and one of its major gauged tributaries, Love Creek, and these areas coincided with lower standard deviations in the water table mapping (Fig. 6). The areas of very shallow water tables (0 m, < 0.25 m, < 0.5 m, < 0.75 m, < 1 m below the ground surface) were tabulated and plotted (Fig. 7a). The percentage changes in "saturated area" (i.e. water tables within a specified depth to surface) between the spring (September–October) peak and autumn (April–May) trough were low in absolute terms (< 0.15 % of area < 100 m in elevation) and relative terms (9–19 % variation between peaks and troughs). An example is shown in Fig. 6 of the difference in the area with the water table at the surface between March and September 2009. In comparison, the mean of the three baseflow time-series (Sect. 3.1) showed relative variations of 72–90 % between peaks and troughs. The saturated areas were restricted to the valley floor of the catchment, indicating little regional groundwater discharge into minor tributaries and this is analysed further in Sect. 3.5.

The relationship between the monthly percentage change in saturated area and the estimated monthly baseflow using the Eckhardt filter was also examined for each year (Fig. 7b). The relationship shows hysteresis with the rising limb generally being steeper and more non-linear compared to the falling limb. The peak saturated area does typically coincide with peak estimated baseflow (except for 2007) but, unexpectedly, years with lower saturated area (e.g. 2010) have higher baseflow for a given saturated area than years with larger saturated areas. This indicates that peak changes in the saturated area are not the dominant driver of peak variations in baseflow, as measured by the Eckhardt filter.

The comparison between monthly changes in saturated volume and mean monthly Eckhardt baseflow (Fig. 8) provides further evidence that the regional groundwater discharge is not the major driver of the baseflow time-series. The baseflow time-series show that peak annual baseflow amount steadily increased between 2008 and 2010, a pattern mirrored by the total streamflow (see Fig. 2). However, over this period the saturated volume changes (at elevations < 100 m) did not show any increasing trend. For months with declining saturated volume changes (i.e. periods where changes in saturated volume are dominated by discharge) we used a specific yield of 0.3 to convert the total volume change to a volume of discharged water. This specific yield value is high (Nwankwor et al., 1984) and so likely provides an upper bound to the groundwater discharge, particularly since any phreatic evapotranspiration flux is not considered. The calculated value of the ratio between the monthly baseflow and the corresponding monthly change in mapped water volume ranged between 0.1 and 20.3, with a mean of 4.4. The late summer to winter period (February to August, $n = 5$) had a mean ratio of 0.6 (i.e. saturated volume change greater than baseflow) while the spring to early summer period (September to January, $n = 13$) had a mean ratio of 7.0 (i.e. saturated volume change ≪ baseflow). These ratios indicate that the monthly baseflow fluxes are significantly larger than can be explained by groundwater discharge during the spring to early summer period and requires a significant additional flux of "slow flow" into the river (see also Fig. 10).

3.5 Relationship between groundwater and tributary chemistry

The relationship between regional groundwater and ungauged tributary chemistry was examined by grouping subcatchments using the depth to water table upstream of each sampling point on the ungauged tributaries. The subcatchment areas ranged from 0.4 to 47.4 km^2 (mean 11.0 km^2) and the seasonal peak water table level in September 2010 was used in the analysis as it was a representative period of seasonal high water table for the study period. The minimum monthly water table depths within the subcatchments ranged between −6 (i.e. above ground surface) to 84 m below ground surface. Given the uncertainty in the minimum mapped position of the water table surface (i.e. see the mapped standard deviation of the water table position in Fig. 6), the subcatchments were arbitrarily divided between those with groundwater within 5 m of the land surface anywhere within the sub-catchment (i.e. where groundwater discharge within the subcatchment was possible) and those with deeper groundwater (Fig. 9).

HESSD
11, 12405–12441, 2014

There were no significant differences in the tributary compositions in subcatchments with shallow groundwater (i.e. minimum water tables < 5 m from the ground surface) or deep groundwater. These results suggest that seasonal regional groundwater table rises are not likely to drive seasonal increases in ungauged tributary inflow from the upper parts of the catchment. This is consistent with the chemistry of the major tributaries being similar to that of the Gellibrand River flow rather than that of the alluvial groundwater (Fig. 3). Therefore, seasonal increases in ungauged tributary inflow are more likely to be driven by interflow or perched aquifer processes, rather than variations in the regional unconfined groundwater. The baseflow filter estimates show large increases in the "slow flow" component of streamflow during winter-spring periods that were not consistent with probable groundwater discharge (Fig. 8). The mass balance calculations indicate that small, ungauged tributaries are a significant contributor to this increase and can be a contributor even during low flow periods.

4 Discussion

4.1 Baseflow estimates

Digital baseflow filters separate out the "slow flow" component of streamflow. As such, they provide an effective upper bound on possible groundwater discharge to streamflow (Cartwright et al., 2014). This was tested by plotting baseflow estimates for the Gellibrand River from digital filter and tracer mass balance analyses (Fig. 10) for the 2011–2013 period. The tracer estimates include the range of estimates from Atkinson et al. (2014) for sampling conducted in 2011–2012 using ^{222}Rn and Cl mass balance plus the results from this study for sampling in 2013 using major ions. None of these estimates are directly comparable as they measure different components of baseflow. The digital filter time-series estimates baseflow from the entire catchment upstream of Bunker Hill gauging station. The Atkinson et al. (2014) estimates are for the groundwater discharge component of streamflow measured over the alluvial valley

Discussion Paper | Discussion Paper | Discussion Paper | Discussion Paper |
HESSD
11, 12405–12441, 2014

Title Page
Abstract | Introduction
Conclusions | References
Tables | Figures
◂ | ▸
Back | Close
Full Screen / Esc
Printer-friendly Version
Interactive Discussion

reach (approximately two thirds of the Bunker Hill to Upper Gellibrand reach, see Fig. 1) and use a two end-member mass balance approach (tributary inflow was not considered). The tracer mass balance results from our study are for the groundwater discharge component of baseflow over the Bunker Hill to Upper Gellibrand reach and account for ungauged tributary inflow. For additional comparison, the 10 day average residual discharge (i.e. Bunker Hill discharge less other gauged tributaries lagged by one day – Upper Gellibrand, Lardner Creek, Love Creek) and the mean daily saturated volume change for months with decreasing volumes were analysed (Sect. 3.4, Fig. 8).

The tracer estimates of groundwater discharge and the residual discharge vary considerably around the digital filter baseflow time-series (Fig. 10). In particular, the residual discharge is larger than the digital filter baseflow during high flow periods but can be lower during low flow periods. The use of a larger BFI_{max} value, consistent with the recommendations of Eckhardt (2005), would increase the digital filter estimates but would also result in more periods of baseflow greater than total streamflow. Tracer data can also be used to calibrate the BFI_{max} parameter (Gonzalez et al., 2009) if a suitable end-member signature can be identified. However, in catchments with low salinity alluvial groundwater (i.e. catchments with low groundwater residence time), end-member differentiation can be an issue (Kendall et al., 2001). For example, the Atkinson et al. (2014) mass balance estimates of groundwater discharge generally cluster around the residual discharge time-series but neither separate out in-reach tributary flow from groundwater discharge. This could be an important distinction for water resource management. The estimate of groundwater volume change (considered as an upper bound estimate due to the use of a high specific yield and not accounting for phreatic evapotranspiration) generally sits below the baseflow and residual discharge estimates.

The different estimates of baseflow and groundwater discharge emphasise the difficulties in separating and defining these important fluxes, particularly how they vary seasonally. In the context of the catchment used in this study, these variations raise questions of whether the in-reach tributary inflow can be lumped with groundwater

HESSD
11, 12405–12441, 2014

discharge (i.e. does regional groundwater discharge also drive tributary flow) and does the digital baseflow filter analysis overestimate groundwater discharge during high flow periods.

4.2 Baseflow – water table dynamics

The first two hypotheses addressed by this paper involve the ability of monthly water table dynamics to explain monthly variations in digital filter estimated baseflow. Large increases in baseflow during the high flow season (e.g. winter-spring) could also contain contributions from other slow fluxes (e.g. interflow and perched aquifer discharge contributing to tributary flow, bank storage return). In order to avoid overestimations of groundwater discharge, it is important to independently test the assumption of a single storage (i.e. regional groundwater) driving baseflow.

In terms of the groundwater contribution, we postulated that the main driver of large increases in baseflow would be non-linear increases in the discharge area as groundwater levels rose and intersected more of the land surface. Monthly water table surfaces were used to test whether such increases in discharge area are a feasible mechanism. In the case of the Gellibrand catchment, the water table data showed that only modest increases in discharge area occurred during the seasonal peaks in groundwater levels and the magnitude of seasonal peaks in this measure showed a poor coincidence with the magnitude of seasonal peaks of digital filter estimated baseflow. Uncertainties in the geostatistically defined groundwater surfaces were not considered to significantly affect the relationship between discharge area and estimated baseflow. Most monitoring bores were located in the valley floors and so confidence in the interpolated water table surfaces was highest in these areas. Consequently, varying the definition of discharge area (i.e. from 0 to 1 m below the ground surface) did not result in large changes (Fig. 7a). However, fluctuations in the water table remain a relatively coarse measure and provide only a first-order estimate of possible groundwater discharge patterns. For instance, the mapping may not have the resolution to identify near-stream zones where capillary fringing effects could lead to large increases in discharge with a small

HESSD
11, 12405–12441, 2014

rise in water content in the unsaturated zone (Gillham, 1984). Furthermore, the spatial correlation (as defined by the model variogram) may vary with the groundwater level (Lyon et al., 2006; Peterson et al., 2011) and alternative external drift terms to land surface elevation, such as topographic wetness index, could possibly better represent near-stream spatial heterogeneity.

The water table mapping technique also assumes that the groundwater–river interaction is dominated by unconfined groundwater. Atkinson et al. (2014) found that much of the estimated groundwater discharge (50–90 %) in the study catchment was occurring over a short 5–10 km reach where the river intersected outcropping Eastern View Formation, the main regional semi-confined aquifer. It is quite possible that variations in discharge from this regional aquifer may not be adequately represented by changes in the unconfined water table. However, temporal changes in the saturated volume of the unconfined groundwater, as estimated by water table mapping, should provide a first order control on the total amount of groundwater discharge. The digital filter estimates of baseflow were generally significantly larger in the spring–early summer period than could be explained by generous estimates of groundwater volume change in these periods. This "excess" baseflow most likely represents interflow and hillslope perched aquifer discharge contributing to streamflow as the catchment drains following the winter–spring wet season.

4.3 End member – water table dynamics

The geostatistical mapping of groundwater surfaces in conjunction with terrain analysis allows the testing of end-member assumptions. For example, streamflow from small tributaries during dry periods could be sourced primarily from regional unconfined groundwater or perched aquifer–interflow type processes. Given the lack of availability of piezometers targeting the latter pathways in most catchments, the capacity to test the possible source of tributary flow provides important information on the suitability of the tributary flow as a separate end-member to flow in the main river. In this context, the results from this study clearly show that much of the small tributary flow in the Gellibrand

HESSD
11, 12405–12441, 2014

catchment has a similar chemical signature to the regional groundwater. Nevertheless, most tributaries were sampled from sub-catchments with regional groundwater significantly deeper than the land surface. The chemical similarities between the small tributary flow (probably representing interflow) and the regional groundwater was not unexpected given that it is likely that this interflow development is the major contributor to the deeper regional groundwater recharge. The ionic similarities between these end-members illustrate that mass balance techniques will struggle to separate these fluxes with any confidence and that additional, independent data, such as water table mapping, are required to confidently identify the groundwater discharge flux.

5 Conclusions

Geostatistical mapping of unconfined groundwater surfaces provides a useful, independent dataset for investigating sources of fluxes contributing to baseflow estimated by traditional digital filter and tracer end-member approaches. In particular, the method can provide added confidence in the lower bound of baseflow estimates that best correspond to regional groundwater discharge in both low and high flow periods. Specifically, the groundwater surface dataset can be used to identify whether variations in discharge area (i.e. groundwater intersecting the land surface) or saturated volume can explain seasonal variations in baseflow, as estimated using digital filters. This dataset is particularly useful in humid, hilly catchments where interflow or perched aquifer discharge is likely to be a significant process and where the different "slow flow" fluxes have similar low salinity chemistry and relatively short residence times. Sufficient monitoring bore data to construct water table maps are not available in all catchments but this method adds significant value to water resource management where these monitoring data are available.

The Supplement related to this article is available online at doi:10.5194/hessd-11-12405-2014-supplement.

Author contributions. J. F. Costelloe, A. W. Western and J. J. McDonnell designed the field experiments and analyses. K. Halbert and T. J. Peterson designed and carried out the water table mapping with T. J. Peterson developing the model code for the temporal interpolation of groundwater observations and mapping of groundwater surfaces. J. F. Costelloe carried out most of the data analysis and prepared the manuscript with contributions from all co-authors.

Acknowledgements. This work is funded by the Australian Research Council Discovery Project scheme through project DP120100253. We greatly appreciate the provision of groundwater chemistry data and introduction to the Gellibrand catchment by Alex Atkinson and Ian Cartwright from Monash University.

References

Atkinson, A. P., Cartwright, I., Gilfedder, B. S., Hofmann, H., Unland, N. P., Cendón, D. I., and Chisari, R.: A multi-tracer approach to quantifying groundwater inflows to an upland river; assessing the influence of variable groundwater chemistry, Hydrol. Process., doi:10.1002/hyp.10122, in press, 2014.

Boezio, M. N. M., Costa, J. F. C. L., and Koppe, J. C.: Kriging with an external drift versus collocated cokriging for water table mapping, T. I. Min. Metall. B, 115, 103–112, 2006.

Cartwright, I., Hofman, H., Sirianos, M. A., Weaver, T. R., and Simmons, C. T.: Geochemical and ^{222}Rn constraints on baseflow to the Murray River, Australia, and timescales for the decay of low-salinity groundwater lenses, J. Hydrol., 405, 333–343, 2011.

Cartwright, I., Gilfedder, B., and Hofmann, H.: Contrasts between estimates of baseflow help discern multiple sources of water contributing to rivers, Hydrol. Earth Syst. Sci., 18, 15–30, doi:10.5194/hess-18-15-2014, 2014.

Chen, X. and Wang, D.: Evaluating the effect of partial contributing storage on the storage-discharge function from recession analysis, Hydrol. Earth Syst. Sci., 17, 4283–4296, doi:10.5194/hess-17-4283-2013, 2013.

Cook, P. G., Favreau, G., Dighton, J. C., and Tickell, S.: Determining natural groundwater influx to a tropical river using radon, chlorofluorocarbons and ionic environmental tracers, J. Hydrol., 277, 74–88, 2003.

Desbarats, A. J., Logan, C. E., Hinton, M., and Sharpe, D. R.: On the kriging of water table elevations using collateral information from a digital elevation model, J. Hydrol., 255, 25–38, 2002.

Eckhardt, K.: How to construct recursive digital filters for baseflow separation, Hydrol. Process., 19, 507–515, 2005.

Eckhardt, K.: A comparison of baseflow indices, which were calculated with seven different baseflow separation methods, J. Hydrol., 352, 168–173, 2008.

Fenicia, F., Savenije, H. H. G., Matgen, P., and Pfister, L.: Is the groundwater reservoir linear? Learning from data in hydrological modelling, Hydrol. Earth Syst. Sci., 10, 139–150, doi:10.5194/hess-10-139-2006, 2006.

Gillham, R. W.: The capillary fringe and its effect on water-table response, J. Hydrol., 67, 307–324, 1984.

Gonzales, A. L., Nonner, J., Heijkers, J., and Uhlenbrook, S.: Comparison of different base flow separation methods in a lowland catchment, Hydrol. Earth Syst. Sci., 13, 2055–2068, doi:10.5194/hess-13-2055-2009, 2009.

Jencso, K. G. and McGlynn, B. L.: Hierarchical controls on runoff generation: topographically driven hydrologic connectivity, geology and vegetation, Water Resour. Res., 47, W11527, doi:10.1029/2011WR010666, 2011.

Jencso, K. G., McGlynn, B. L., Gooseff, M. N., Wondzell, S. M., Bencala, K. E., and Marshall, L. A.: Hydrologic connectivity between landscapes and streams: transferring reach- and plot-scale understanding to the catchment scale, Water Resour. Res., 45, W04428, doi:10.1029/2008WR007225, 2009.

Kendall, C., McDonnell, J. J., and Gu, W.: A look inside “black box” hydrograph separation models: a study at the Hydrohill catchment, Hydrol. Process., 15, 1877–1902, 2001.

Leblanc, M., Tweed, S., Van Dijk, A., and Timbal, B.: A review of historic and future hydrological changes in the Murray-Darling Basin, Global Planet. Change, 80–81, 226–246, 2012.

Li, L., Maier, H. R., Partington, D., Lambert, M. F., and Simmons, C. T.: Performance assessment and improvement of recursive digital baseflow filters for catchments with different physical characteristics and hydrological inputs, Environ. Modell. Softw., 54, 39–52, 2014.

Llamas, M. R. and Martínez-Santos, P.: Intensive groundwater use: silent revolution and potential source of social conflicts, J. Water Res. Pl.-ASCE, 131, 337–341, 2005.

HESSD
11, 12405–12441, 2014

Lyon, S. W., Seibert, J., Lembo, A. J., Walter, M. T., and Steenhuis, T. S.: Geostatistical investigation into the temporal evolution of spatial structure in a shallow water table, Hydrol. Earth Syst. Sci., 10, 113–125, doi:10.5194/hess-10-113-2006, 2006.

McCallum, J. L., Cook, P. G., Brunner, P., and Berhane, D.: Solute dynamics during bank storage flows and implications for chemical base flow separation, Water Resour. Res., 46, W07541, doi:10.1029/2009WR008539, 2010.

McGlynn, B. L. and McDonnell, J. J.: Quantifying the relative contribution of riparian and hillslope zones to catchment runoff, Water Resour. Res., 39, 1310, doi:10.1029/2003WR002091, 2003.

Meshgi, A., Schmitter, P., Babovic, V., and Chui, T. F. M.: An empirical method for approximating stream baseflow time series using groundwater table fluctuations, J. Hydrol., 519, 1031–1041, doi:10.1016/j.jhydrol.2014.08.033, 2014.

Nathan, R. J. and McMahon, T. A.: Evaluation of automated techniques for base flow and recession analyses, Water Resour. Res., 26, 1465–1473, 1990.

Nwankwor, G. I., Cherry, J. A., and Gillham, R. W.: A comparative study of specific yield determinations for a shallow sand aquifer, Ground Water, 22, 764–772, 1984.

Perrin, J., Mascré, C., Pauwels, H., and Ahmed, S.: Solute recycling: an emerging threat to groundwater quality in southern India, J. Hydrol., 398, 144–154, 2011.

Peterson, T. J. and Western, A. W.: Nonlinear time-series modeling of unconfined groundwater head, Water Resour. Res., doi:10.1002/2013WR014800, in press, 2014.

Peterson, T. J., Cheng, X., Western, A. W., Siriwardena, L., and Wealands, S. R.: Novel indicator geostatistics for water table mapping that incorporate elevation, land use, stream network and physical constraints to provide probabilistic estimation of heads and fluxes, in: Proceeding of the 19th International Congress on Modelling and Simulation, Perth, Australia, 12–16 December 2011, 3910–3916, 2011.

SKM: Newlingrook groundwater investigation – Gellibrand River streambed and baseflow assessment, Report to Barwon Water, Geelong, Australia, available at: http://www.barwonwater.vic.gov.au/vdl/A5711327/Newlingrook groundwater investigation - Gellibrand River streambed and baseflow assessment (report by SKM consultants).pdf (last access: 21 January 2014), 2012.

Sophocleous, M.: From safe yield to sustainable development of water resources – the Kansas experience, J. Hydrol., 235, 27–43, 2000.

Sophocleous, M.: Interactions between groundwater and surface water; the state of the science, Hydrogeol. J., 10, 52–67, 2002.
Tallaksen, L. M.: A review of baseflow recession analysis, J. Hydrol., 165, 349–370, 1995.
van Dijk, A. I., Beck, H. E., Crosbie, R. S., de Jeu, R. A., Liu, Y. Y., Podger, G. M., Timbal, B., and Viney, N. R.: The Millennium Drought in southeast Australia (2001–2009): natural and human causes and implications for water resources, ecosystems, economy, and society, Water Resour. Res., 49, 1040–1057, doi:10.1002/wrcr.20123, 2013.
Ward, R. C. and Robinson, M.: Principles of Hydrology, 4th Edn., McGraw-Hill, New York, 2000.
Wittenberg, H.: Baseflow recession and recharge as nonlinear storage processes, J. Hydrol., 219, 20–33, 1999.
Wittenberg, H. and Sivapalan, M.: Watershed groundwater balance estimation using streamflow recession analysis and baseflow separation, Hydrol. Process., 13, 715–726, 1999.
Woessner, W. W.: Stream and fluvial plain ground water interactions: rescaling hydrogeologic thought, Ground Water, 38, 423–429, doi:10.1111/j.1745-6584.2000.tb00228.x, 2000.

Table 1. Estimates of groundwater discharge (Q_{gw}) and ungauged tributary discharge (Q_{ut}) using mass balance analysis. Q_{res} is the residual discharge after accounting for the gauged discharges within the study catchment.

Date	Q_{gw} ($ML\,d^{-1}$)	Q_{ut} ($ML\,d^{-1}$)	Q_{res} ($ML\,d^{-1}$)	Tracer	Method
21 Jan 2013	14.5	2.3	16.8	Cl–Ca	Two end-member
21 Jan 2013	11.4	5.4	16.8	Cl–Mg	Two end-member
21 Jan 2013	15.9	0.9	16.8	Ca–Mg	Two end-member
21–28 Jan 2013	13.7	1.8	15.5	Cl	One end-member series*
21–28 Jan 2013	7.1	8.4	15.5	Na	One end-member series
21–28 Jan 2013	13.7	1.8	15.5	Ca	One end-member series*
21–28 Jan 2013	13.7	1.8	15.5	Mg	One end-member series*
21–28 Jan 2013	4.7	10.8	15.5	^{18}O	One end-member series
21–28 Jan 2013	8.1	7.5	15.5	^{2}H	One end-member series
7 Jun 2013	25.2	59.6	84.8	Cl–Na	Two end-member
7 Jun 2013	48.8	36.0	84.8	Na–Mg	Two end-member
7 Jun 2013	38.2	46.6	84.8	Cl–Ca	Two end-member
7 Jun 2013	68.9	15.9	84.8	Cl–Mg	Two end-member
7 Jun 2013	9.8	75.0	84.8	Na–Ca	Two end-member
20 Jun 2013	14.7	31.0	45.7	Cl–Na	Two end-member
20 Jun 2013	42.4	3.3	45.7	Na–Mg	Two end-member
18–20 Jun 2013	51.9	0.3	52.2	Cl	One end-member series*
18–20 Jun 2013	0.0	52.2	52.2	Cl–Na	Two end-member series*
18–20 Jun 2013	51.9	0.3	52.2	Ca–Mg	Two end-member series*
18–20 Jun 2013	0.0	52.2	52.2	Na–Mg	Two end-member series*
16 Dec 2013	5.3	30.6	35.8	Na–Ca	Two end-member
16 Dec 2013	17.1	18.7	35.8	Cl–Ca	Two end-member

* Solution poorly constrained.

HESSD
11, 12405–12441, 2014

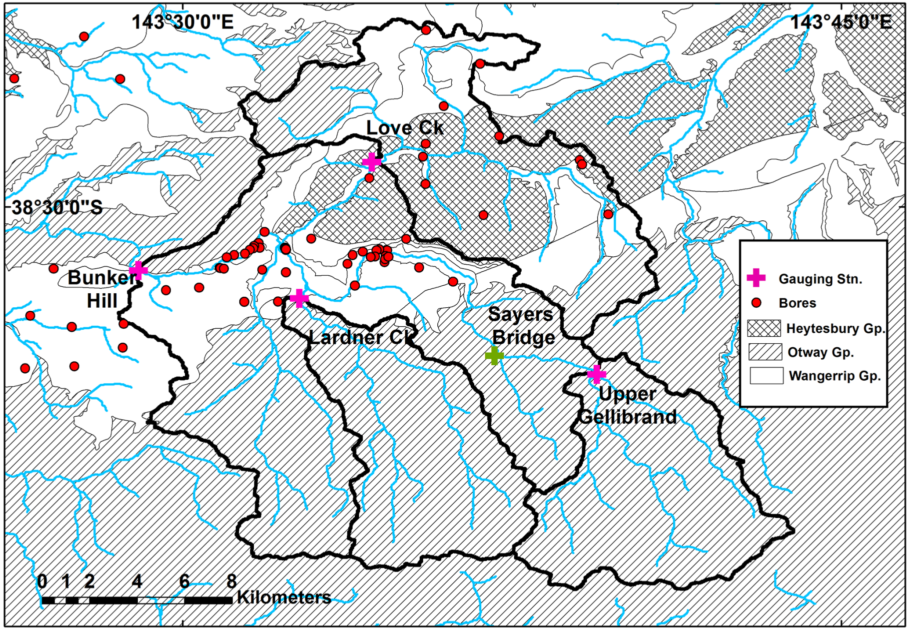

Figure 1. Location and geology of Gellibrand River catchment in Victoria, Australia showing catchment and gauged subcatchment boundaries, monitoring bores, gauging stations and Sayers Bridge (ungauged) river sampling location.

HESSD
11, 12405–12441, 2014

Groundwater surface mapping informs sources of catchment baseflow

J. F. Costelloe et al.

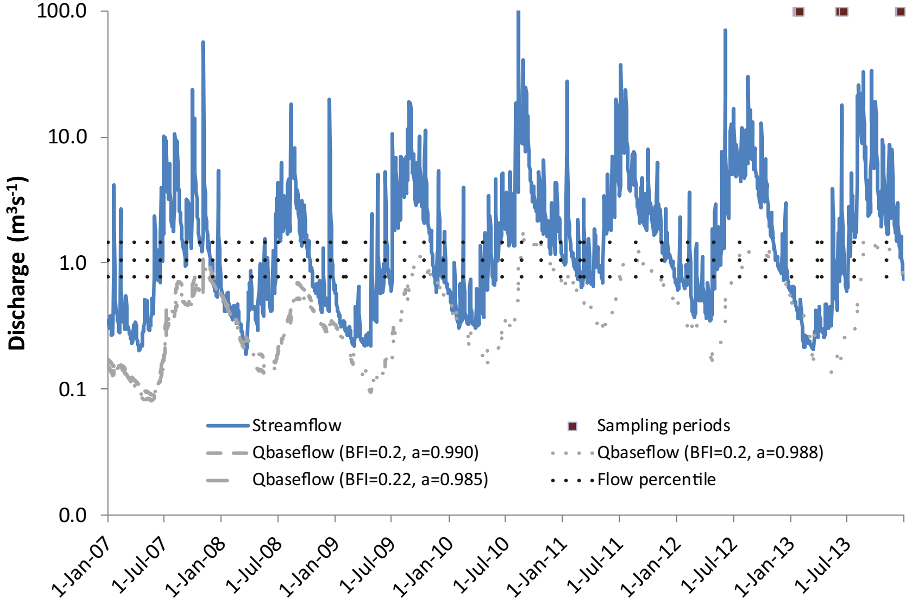

Figure 2. Hydrograph at Bunker Hill gauging station (235227) illustrating the seasonality of flow. The 30th, 40th and 50th percentiles of flow based on the entire record (1979–2013) are shown along with periods of streamflow hydrochemical sampling. Three baseflow separation hydrographs generated using different parameter values for the Eckhardt filter are displayed.

HESSD
11, 12405–12441, 2014

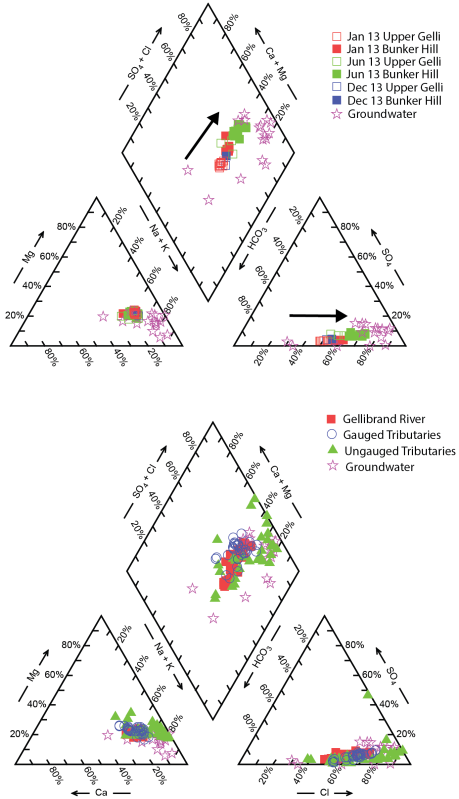

Figure 3. Piper diagrams showing temporal and spatial patterns in the chemistry of streamflow and groundwater. The top panel shows seasonal variations in composition of flow in the Gellibrand River at the upstream (Upper Gellibrand) and downstream (Bunker Hill) sites over three sampling trips. The internal arrows show direction of compositional change from upstream to downstream and also from summer to winter towards the general groundwater composition. The lower panel shows compositional differences across all sampling trips between Gellibrand River, gauged tributaries, ungauged tributaries and groundwater.

HESSD
11, 12405–12441, 2014

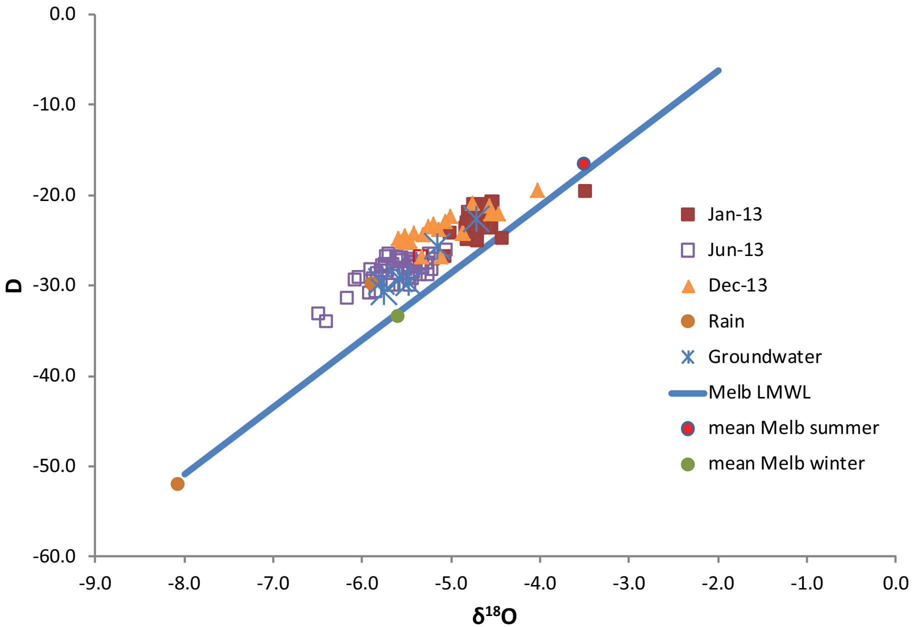

Figure 4. Stable isotope data for streamflow and groundwater samples from three sampling trips (January, June and December 2013). The local Meteoric Water Line (LMWL) for Melbourne is shown for comparison (Global Network of Isotopes in Precipitation data).

HESSD
11, 12405–12441, 2014

HESSD
11, 12405–12441, 2014

Groundwater surface mapping informs sources of catchment baseflow

J. F. Costelloe et al.

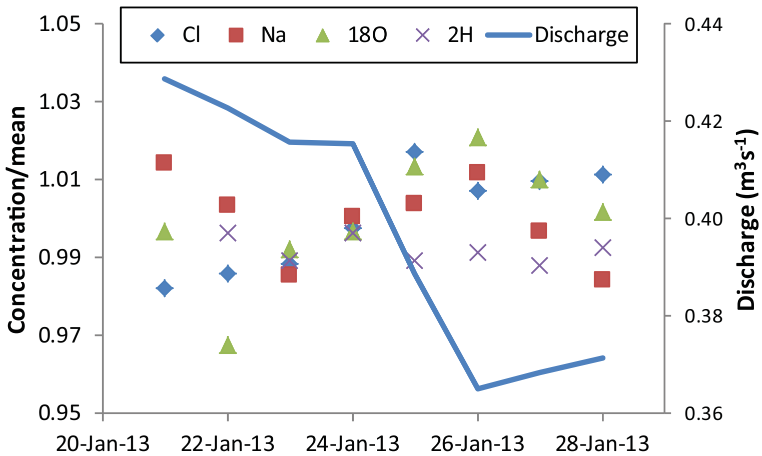

Figure 5. Stable isotope and major ion changes during streamflow recession of January 2013 measured at Bunker Hill gauging station. Concentrations are divided by the mean concentration of the sampling period for each tracer.

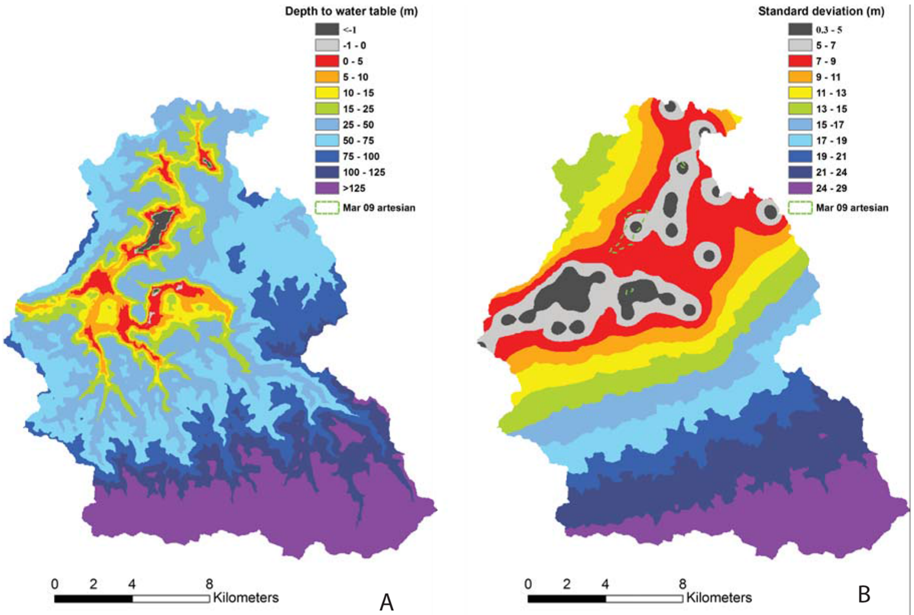

Figure 6. Depth to water table map **(a)** and kriging standard deviation **(b)** for 1 September 2009. Areas of shallow or intersecting (artesian) water table are restricted to the Gellibrand River (centre) and Love Creek (north) valley floors. The variations in artesian water table areas between shallower (September) and deeper (March) water tables are relatively minor.

HESSD
11, 12405–12441, 2014

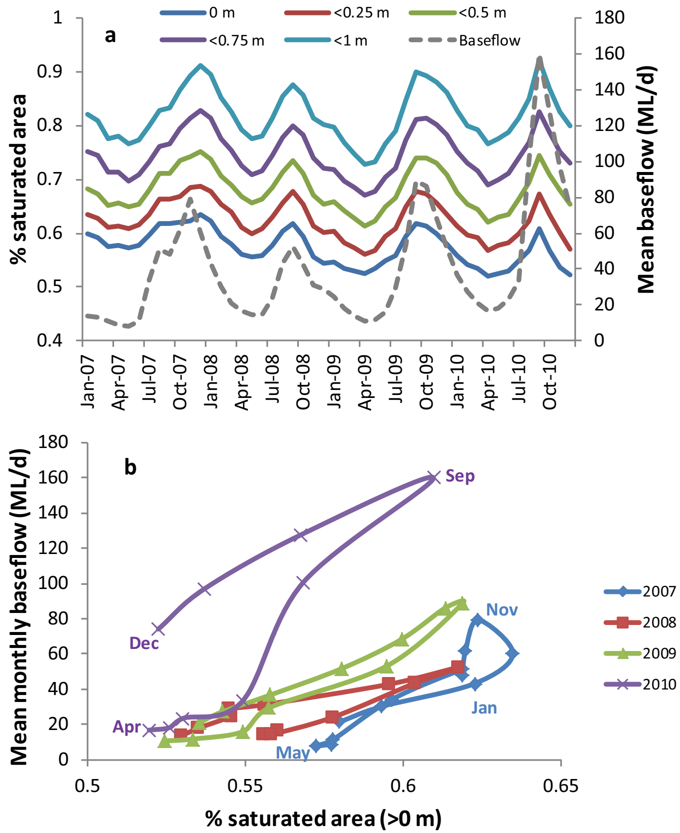

Figure 7. (a) Percentage saturated area (intersection of groundwater surface with land surface) variations over time. The position of the water table is shown for five depths (0–1 m) to allow for uncertainties in the mapping of the depth to water table. **(b)** Variations in percentage saturated area against mean monthly baseflow calculated from the three time-series generated using the Eckhardt baseflow filter for the Bunker Hill gauging record.

HESSD
11, 12405–12441, 2014

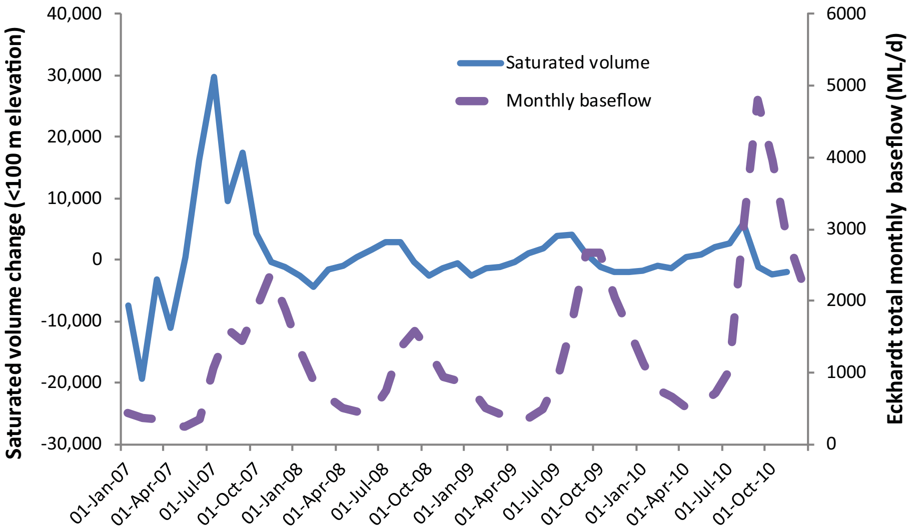

Figure 8. Monthly variations in saturated volumes for the catchment area with elevation < 100 m and for monthly baseflow derived from Eckhardt analysis.

HESSD
11, 12405–12441, 2014

Groundwater surface mapping informs sources of catchment baseflow

J. F. Costelloe et al.

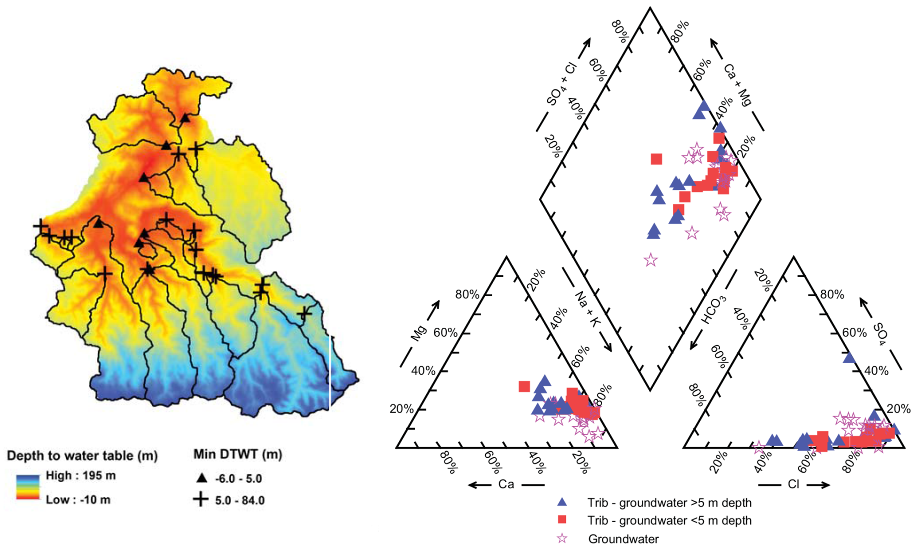

Figure 9. Piper diagram (right) shows tributary samples grouped by the minimum depth to groundwater table in the sub-catchment upstream of the sampling point. Compositions of sampled groundwater bores are also shown. The spatial location and sub-catchment extent are shown superimposed on the depth of water table map for September 2010.

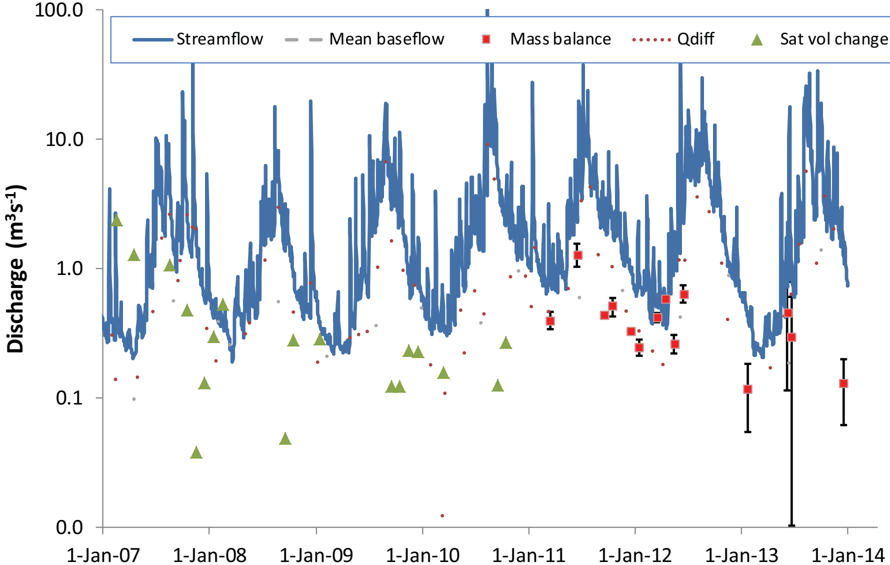

Figure 10. Hydrograph at Bunker Hill gauging station (235227) showing various estimates of baseflow and groundwater discharge. The Bunker Hill discharge and mean estimate of baseflow using three sets of parameter values for the Eckhardt filter are as shown in Fig. 2. Also shown is the 10 day mean residual discharge at Bunker Hill (Q_{diff}) after accounting for all gauged tributary inflow (lagged by one day) and the mean monthly saturated volume change (as shown in Fig. 8). The midpoint and range of estimates of groundwater discharge from tracer analysis are shown for 2011–2012 (Atkinson et al., 2014) and 2013 (this study).